

Beam and target optimization for energy production in accelerator driven systems

Mihaela Paraipan^{1,2,*}, Anton A. Baldin^{1,3}, Elina G. Baldina^{1,3}, and Serguey I. Tyutyunikov¹

¹Joint Institute of Nuclear Research, Dubna, Russia

²Institute of Space Science, Bucharest-Magurele, Romania

³Institute for Advanced Studies "OMEGA", Dubna, Russia

Abstract. The new concept of light nuclear beams instead of proton beams for ADS is substantiated. The influence of the target structure on the energy efficiency of 0.5-4 GeV proton beams and 0.25 – 0.5 AGeV light ion beams is studied. The target consists of rods with different composition (metal, oxide, carbide) and different levels of enrichment in order to implement the target with a criticality coefficient of 0.96 -0.97, which ensures safe operation. The cooling with different metals (lead, lead-bismuth eutectic - LBE, and sodium) is compared. The use of converters from very light materials (lithium, beryllium, carbon) and their influence on the neutron spectrum and energy released are analysed.

1 Introduction

An accelerator driven system (ADS) presents some advantages in comparison with a classical nuclear reactor such as safer exploitation, higher level of burning of minor actinides, and the transmutation of long lived isotopes. The design of an ADS must retain these advantages and maximize the energy efficiency. In the previous works the authors demonstrated that light ion beams have a superior energy efficiency for ADS as compared to protons [1, 2]. These conclusions were obtained in quasi-infinite natural and enriched uranium targets. In the present paper targets with more realistic structure are analysed.

2 Method

The energy efficiency of a beam is characterized by the gain factor G defined as the ratio of the electrical power produced in the irradiated target P_{prod} to the power spent to accelerate the beam P_{spent} .

The power produced depends on the energy released in the target per incident projectile E_{dep} , beam intensity I_{beam} , and conversion coefficient from thermal to electrical power η_{el} :

$$P_{prod} = E_{dep} \cdot I_{beam} \cdot \eta_{el}. \quad (1)$$

The energy released in the target was calculated via simulation with the code Geant4 [3]. The reliability of the predictions obtained with Geant4 was verified using experimental data

*e-mail: mihaela_paraipan@yahoo.com

on neutron yield from thin and thick metallic targets [4], and the conclusion was made that one can rely on the results of the simulations within 25%. Standard electromagnetic models were used to model the electromagnetic interaction. The inelastic interaction was simulated with the cascade models (Bertini cascade for hadrons and pions, binary cascade for ions). For neutrons with an energy below 20 MeV high precision neutron models, based on a detailed implementation of the experimental data from ENDF library were used. A value of 0.4 was used for η_{el} .

The interaction of proton beams with an energy 0.5-4 GeV, and light ion beams (${}^7\text{Li}$, ${}^9\text{Be}$, ${}^{12}\text{C}$) with an energy of 0.25 – 1 AGeV was simulated in targets with various geometries and composition. The target is an assembly of fuel rods in a bath of coolant. Different types of uranium and thorium fuel were analysed: metallic alloy with Zr, oxide and carbide. The following parameters were varied: the radius r of the fuel rods (between 0.5-1 cm), the length L of the rods (between 100-150 cm), the distance d between rods (between 1-5 cm), the total radius R of the fuel assembly (between 70-90 cm). In each case the level of enrichment was properly chosen in order to implement a target with criticality coefficient $k_{eff}=0.96$ -0.97. Metals Pb, Pb-Bi eutectic (LBE) and Na were used as coolant. The influence of the target geometry and composition on the neutron spectrum and on the ratio between the energy released by different ions was studied.

The power spent to accelerate the beam was calculated with the method presented in detail in [2]. Here we make only a short description. P_{spent} includes the power transmitted to the beam P_{beam} (which depends on the ion mass number A , the final energy per nucleon E , and the beam intensity) and the power necessary to maintain the functioning of the accelerator P_{acc} . For a linear accelerator this last term depends on the accelerator length and scales as $A \cdot E/Z$ where Z is the atomic number of the ion. In this way if P_{spent0} and the accelerator efficiency η_0 for a reference particle (atomic number Z_0 , mass number A_0 , final energy per nucleon E_0) are known one can calculate the power spent for another particle. Assuming the same beam intensity the one gets:

$$P_{spent} = P_{beam} + P_{acc} = A \cdot E_0 \cdot I_{beam} + \frac{A \cdot Z_0 \cdot E}{A_0 \cdot Z \cdot E_0} P_{spent0} (1 - \eta_0). \quad (2)$$

Proton with energy 1.5 GeV (energy at which protons accelerated in a linac have the maximum energetic efficiency [1]) was used as reference particle. A value of 0.18 for the total accelerator efficiency for the reference particle was considered. Such high value is not achieved yet, still is planned to be realized at European Spallation Source (ESS) project. The value used for the beam intensity was $1.25 \cdot 10^{16}$.

3 Results and discussion

The variations in the target geometry and fuel composition do not modify the shape of the neutron spectrum and preserve the ratio between the energy deposited by different ions. Some values for the energy deposited per incident particle for beams of ${}^7\text{Li}$ with energy 0.35 and 0.45 AGeV, and protons with energy 1.5 GeV are presented in Tab. 1.

The metallic coolant does not modify the shape of the neutron spectrum either. The energy released obtained with 0.35 AGeV ${}^7\text{Li}$ and 1.5 GeV proton beams in U target cooled with Pb, LBE, and Na are given in Tab. 2. The ratio between the energy released realized with ${}^7\text{Li}$ and proton is preserved. It should be pointed out that Pb or LBE act as better reflectors for neutrons in comparison with Na. If Na is used as coolant the energy released decreases, and the neutron leakage increases from 15% with coolant Pb or LBE to 25% with Na. If one use Na as coolant, one needs to increase the level of enrichment or to use an additional reflector layer in order to obtain the same k_{eff} .

Table 1. The energy released per incident projectile for different target geometries and compositions. The projectile energy is given in AGeV

Dimensions cm	Composition	E_{dep} ^7Li 0.35 MeV/p	E_{dep} ^7Li 0.45 MeV/p	E_{dep} P 1.5 MeV/p
L120R70r0.5d2	U-Pu-Zr 11 % Pu239	9.584e4	1.437e5	1.342e5
L150R90r0.5d2	U-Pu-Zr 9.2 % Pu239	1.031e5	1.567e5	1.536e5
L150R90r0.5d2	Carbide 11.2 % Pu239	9.276e4	1.457e5	1.375e5
L150R90r0.5d2	Oxide 12.3 % Pu239	1.011e5	1.496e5	1.425e5
L150R90r0.5d2	Th-Pu-Zr 13.6 % Pu239	9.423e4	1.429e5	1.381e5

Table 2. The energy released per incident projectile in U target 14.7% U235 irradiated with 0.35 AGeV ^7Li and 1.5 GeV proton beams for Pb, LBE and Na coolants

Projectile	LBE	Pb	Na	Na+20.5% U235
^7Li	1.212e5	1.179e5	2.728e4	1.2289e5
proton	1.948e5	1.848e5	4.561e4	1.814e5

Table 3. The net power production and the energy gain for proton and light ion beams in U target with k_{eff} 0.97 and converters from LBE and Be

Projectile	LBE		Be		
	Energy AGeV	Net power MW	G	Net power MW	
p	1.5	127	8.1	193.3	11.7
^7Li	0.3	62.2	6.5	174.3	16.6
	0.35	87.2	7.7	227.6	18.4
	0.4	113.8	8.6	295	20.7
	^9Be	0.3	51.4	5.3	175.7
^9Be	0.35	77	6.4	241	18
	0.4	105.1	7.5	306.1	19.9
	^{12}C	0.75	389.7	12.8	847.2

The shape of the neutron spectrum is influenced by the material used for the converter. Converters from light materials as Li, Be, or C are useful especially when the target is irradiated with light ion beams with low energy. The energy released increases 1.4 - 3 times. The best results are obtained with Be converter. Two effects contribute to the increase of the energy deposited in the target. On the one hand, materials with low mass number slow the neutrons and determine an increase of the low energy tail in the neutron spectrum. This effect appears for all projectiles and explains the growth of the deposited energy even with proton beams. The effect is more pronounced in targets with high level of enrichment. On the other hand the use of low Z materials produces a significant increase of the range for low energy light ions. As a consequence, the probability to interact inelastically at higher energies increases, and the result is an increased yield of high energy neutrons. The effect of converters on the neutron spectrum is exemplified in Fig. 1. The neutron spectra in targets with converters from LBE and Be irradiated with a beam of ^7Li with energy 0.35 AGeV are presented.

The comparison between the net power production and the energy gain realized with protons and light ion beams in U target with $k_{eff}=0.97$ is given in Tab. 3. The results are similar with those obtained in quasi-infinite target. The optimal energy for protons is ~ 1.5

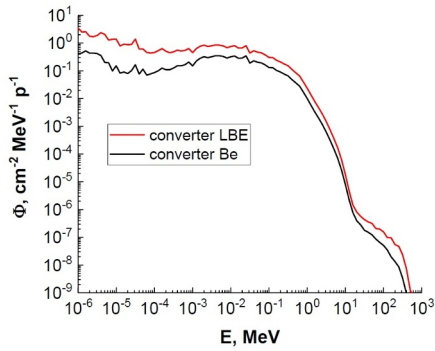


Figure 1. The neutron spectrum in enriched U-Pu target with LBE and Be converters irradiated with 0.35 AGeV ${}^7\text{Li}$ beam

GeV. In the case of a target with converter LBE irradiated with beams of ${}^7\text{Li}$ or ${}^9\text{Be}$ with an energy of 0.4 AGeV one gets almost the same net power production as with 1.5 GeV proton beam, but with significantly higher energy gain G . For Be converter ${}^7\text{Li}$ or ${}^9\text{Be}$ beams with an energy of 0.35 AGeV become equivalent to 1.5 GeV proton beams from the point of view of the net power produced. Another important factor is that the acceleration of ${}^7\text{Li}$ or ${}^9\text{Be}$ at energies 0.35-0.4 AGeV requires accelerators with lower dimensions. We note also, that a ${}^{12}\text{C}$ beam with an energy of 0.75 AGeV requires an accelerator with the same length as 1.5 GeV protons, but produces 3-4 times higher net power.

One has apparently a large liberty in the choice of the target material and geometry. The choice of the optimal configuration, however, must preserve the main advantages of ADS: safe exploitation and deep level of burning of minor actinides. A safe exploitation is ensured if k_{eff} is maintained below 0.99 during the irradiation. The evolution in time of the number of fissions after stopping the beam is presented in the right side of the Fig. 2 for three values of k_{eff} 0.95, 0.97, and 0.986. For k_{eff} below 0.99, the number of fissions decreases by more than 10 times in the first 100 ns from the moment at which the beam is stopped. Such quick response eliminates the risk of an accident. Until now, only the situation at the beginning of the irradiation was analysed. During the irradiation the target composition and k_{eff} change. For the study of the evolution, the target was divided in zones with more or less equal fluence and the change in its composition was calculated for each zone. A schematic representation of the target divided in zones is shown in the left-hand side of Fig. 2. The evolution of the composition depends on the initial level of enrichment. We exemplify for two U-Pu targets with initial value of $k_{eff}=0.97$. The first target with lower dimensions has the initial level of enrichment 11% ${}^{239}\text{Pu}$. The second has higher dimensions and an enrichment of 9.2% ${}^{239}\text{Pu}$. The time dependence of the concentration of ${}^{238}\text{U}$ and ${}^{239}\text{Pu}$ in the central part of the target (zone0 in Fig. 2) is presented in Fig. 3. The central part was chosen because there the largest variations are registered. At refuelling time, rods from this zone must be replaced. We choose the moment when the energy released in the target decreases with 30% from the initial value as the criterion for refuelling. These moments are shown by vertical lines in the figure. The target was irradiated with a beam of ${}^7\text{Li}$ with energy 0.35 AGeV and intensity $1.25 \cdot 10^{16}$.

In the case of the target with enrichment 11% ${}^{239}\text{Pu}$ the concentration of ${}^{239}\text{Pu}$ continuously decreases in time. The energy deposited and k_{eff} slowly decrease, also. Such target does not need control rods during operation. It needs to be refuelled after 900 days. By the moment of refuelling, 7.7% from the initial mass of actinides was burned in the zone 0, and 4% in the zone 3. The concentration of ${}^{239}\text{Pu}$ in the second target has a different evolution: a period of build-up when the k_{eff} rises, followed by a slower decrease. This target needs the use of the control rods during operation. With a proper adjustment of the number of control rods, the fluence, the k_{eff} and the energy released can be kept constant. This is illustrated

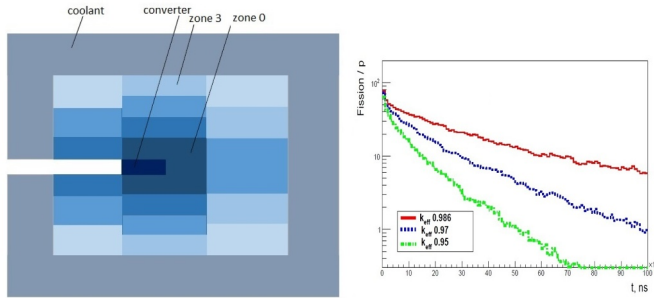


Figure 2. The scheme of the target (left), and the evolution in time of the number of fission when the beam is stopped, in targets with different k_{eff} (right)

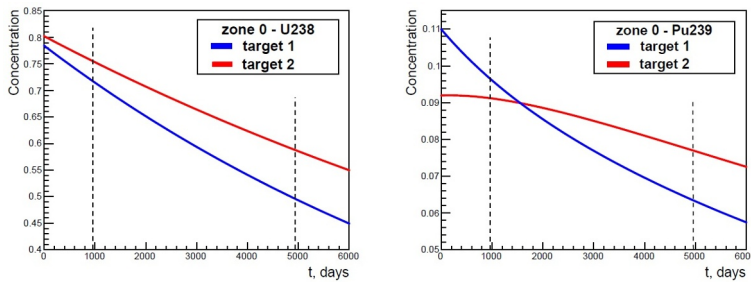


Figure 3. The time dependence of the concentration of ^{238}U (left), and ^{239}Pu (right) in targets with enrichment 9.2% ^{239}Pu and 11% ^{239}Pu irradiated with 0.35AGeV ^7Li beam with an intensity of $1.25 \cdot 10^{16}$

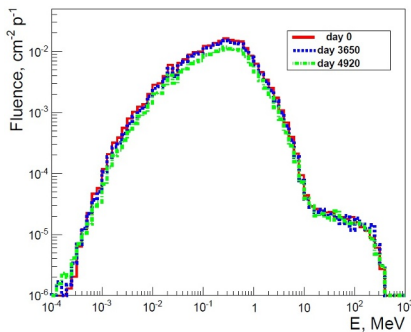


Figure 4. The neutron spectrum in the central part of the target at different periods of irradiation for a target with 9.2% ^{239}Pu irradiated with 0.35 AGeV ^7Li beam with an intensity of $1.25 \cdot 10^{16}$

in the Fig. 4 where the neutron fluence in zone 0 is shown at the beginning of the irradiation, after 10 years, and in the moment of refuelling. For the second target the refuelling is necessary after ~ 5000 days. At this moment 23.4% from the initial mass of actinides was burned in zone 0, and 11.2% in zone 3. If a target with 8.9% ^{239}Pu is used, the mass of the actinides burned in the central region reaches 30%. It is preferable to use a target with lower enrichment which ensures a higher level of fuel burning. The variation of k_{eff} in time is slow, and it does not present any difficulty to control and keep it at safe level.

Thorium targets were also analysed. The shape of the neutron spectrum and the ratio between the energy deposited by different ions are the same as in uranium targets (see Tab. 1). However, for a given geometry a thorium target needs higher enrichment if one intends to obtain the same k_{eff} as in a uranium target. For example, in the geometry L150R90r0.5d2,

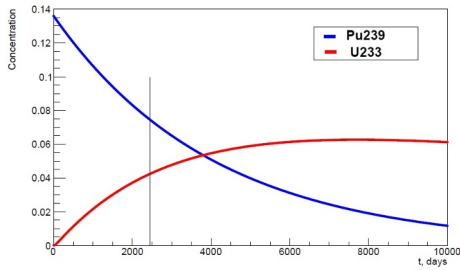


Figure 5. The time dependence of the concentration of ^{239}Pu and ^{233}U , in Th-Pu target with 13.6% ^{239}Pu , irradiated with a beam of ^7Li with energy 0.35 AGeV and intensity $1.25 \cdot 10^{16}$

for $k_{eff}=0.97$ an U-Pu target needs 9.2% ^{239}Pu , while a Th-Pu target requires 13.6% ^{239}Pu . During irradiation, the decrease in the ^{239}Pu concentration is partially compensated by the accumulation of ^{233}U . The difference in the mean values for fission cross section of ^{233}U and ^{239}Pu , which are 2.38 b and 1.66 b, respectively, contributes to the compensation. The time dependence of the concentration for these two isotopes is presented in Fig. 5. The considered beam was ^7Li with an energy of 0.35 AGeV and an intensity of $1.25 \cdot 10^{16}$. The moment of refuelling is shown by vertical line. We remark that the period is about one half of the corresponding period for U-Pu target.

4 Conclusions

Light ion beams ^7Li and ^9Be with energies above 0.3 AGeV, or ^{12}C with an energy higher than 0.5 AGeV demonstrate a superior energy efficiency for energy production in ADS, as compared to protons. The effect is present in both U and Th targets. The fuel composition and target geometry do not influence the ratio between the energy released by different ions, keeping unchanged the shape of the neutron spectrum. Converters from very light materials, in particular Be increase the energy released. The effect is more pronounced for light ions with low energy. Targets with higher dimensions and lower enrichment are preferable because they ensure large periods between refuelling and an increased burning of actinides. Thorium targets need higher enrichment, as compared to U targets with the same geometry and the same k_{eff} . The period for refuelling is shorter for Th targets.

References

- [1] A. A. Baldin, A. I. Berlev, M. Paraipan, S. I. Tyutyunikov, Phys. Part. Nucl. Lett. **14**, 113-119 (2017)
- [2] A. A. Baldin, E. G. Baldina, M. Paraipan, S. I. Tyutyunikov, Ann. Nucl. En. **110**, 973-978 (2017)
- [3] S. Agostinelli et al., Nucl. Instrum. Methods A. **506**, 250–303 (2003)
- [4] A. A. Baldin, A. I. Berlev, I. V. Kudashkin, G. Mogildea, M. Mogildea, M. Paraipan, S. I. Tyutyunikov, Phys. Part. Nucl. Lett. **32**, 391-402 (2016)